Studies of the Reactions of Ferric Iron with Glutathione and some Related Thiols

MAZEN Y. HAMED, JACK SILVER* and MICHAEL T. WILSON*

Department of Chemistry, University of Essex, Wivenhoe Park, Colchester, CO4 3SQ, U.K.

Received July 1, 1982

The anaerobic reactions of ferric salts with glutathione and related thiols have been studied by Mössbauer spectroscopy and fast reaction kinetic techniques. In all cases the final product contains iron(II). Kinetic experiments show the presence of blue intermediate(s) on the reaction pathway. These results are discussed in terms of an overall scheme, and possible binding sites on the thiols are proposed.

Introduction

Glutathione (γ-glutamyl-L-cysteinyl glycine) (1) is ubiquitous in nature and is found in all living cells in relatively high concentrations [1, 2]. There have been many studies on the chelation properties of glutathione with metal ions [2–5]. Amongst these studies there have been a number involving iron(III) [3–5]. The predominant glutathione isomer (1) at physiological pH values possesses eight potential binding sites: two carboxylic acid groups, an amino group, a sulfhydryl group and two amide functions. As all binding sites cannot be simultaneously coordinated to a single metal ion, the coordination chemistry of glutathione is characterised by formation of protonated and polynuclear complexes [2, 3].

Mössbauer studies of the binding reaction of iron(III) to glutathione have clearly demonstrated the production of iron(II). For example, Raudsepp (1975) [5] reports spectra obtained from frozen solutions containing iron(III) and glutathione in which iron(II) was identified at low pH values [5]. Iron(III) chelation by glutathione over a wide pH range has also been studied by Hamed *et al.*, and rapid reduction of the metal was found to occur at low pH [3].

In order to investigate more fully the binding and redox reactions which occur between glutathione and iron(III) we have undertaken both Mössbauer and stopped-flow kinetic experiments. We have also performed parallel studies substituting a variety of thiol compounds for glutathione.

Our kinetic studies have allowed us to identify a coloured (blue) intermediate in the reaction path between iron(III) and all the ligands employed. We have exploited this absorption band (centred at 625 nm) to measure the rate of initial ligand binding to iron and the apparent binding constant for this first step. Comparison of these apparent binding constants together with the calculated extinction coefficients for the intermediates formed starting with glutathione (GSH), cysteine, N-acetyl cysteine, cysteine methyl ester and mercaptoethanol have also allowed us to draw conclusions regarding the nature of the ligands involved in the rapid binding of iron.

Mössbauer studies conducted on solutions frozen either during the course of the reaction (in an attempt to trap the intermediate(s)), or when the reaction had come to completion are also discussed. These studies permit us to identify the step in the reaction in which the formal valence state of the iron changes. We discuss these kinetic and spectral results in terms of an overall scheme.

Experimental

Anhydrous glutathione [reduced crystalline (Sigma)], anhydrous L-cysteine [free base (Sigma)], N-acetyl-L-cysteine (Fluka), anhydrous L-cysteine methyl ester hydrochloride (Sigma), anhydrous glutathione [oxidised form, grade II (Sigma)], mercaptoethanol (Sigma), anhydrous iron(III) chloride (SLR, Fisons), iron(III) nitrate·$9H_2O$ (AR, Fisons), and $FeCl_2 \cdot 4H_2O$ freshly prepared in house were used without further purification.

Stopped-flow Experiments

A weighed amount of the ligand was dissolved in conductivity water, the pH was adjusted to the pH value required; the same procedure was repeated with the iron salt, the solutions were degassed and

*Authors to whom correspondence should be addressed.

0020-1693/83/0000-0000/$03.00

TABLE 1. Mössbauer Parameters from Spectra Obtained on Frozen Solutions of $FeCl_3$ and GSH at Different Stoichiometries at 80 K.

Mixture	pH	δ mm s^{-1}	Δ mm s^{-1}	Γ mm s^{-1}	%A	Iron valence present
$FeCl_3$/GSH (1:1)	2.3	1.41(1)	3.11(1)	0.34(1)	100 ± 3.1	Fe^{2+}
[Fe] = 0.15 *M*						
$FeCl_3$/GSH (2:1)*	1.9	1.41(1)	3.13(0)	0.39(1)	69.7 ± 2.6	Fe^{2+}
		0.57(2)**	*ca.* 0	0.64(5)	30.3 ± 2.6	Fe^{3+}

*Note the difference in the iron(III) non reacted site above, and the new iron(III) site in Spectra 8 and 9 (Table II). **Fe(III) site by comparison with data references 10 and 11 suggest $FeCl_3$ in frozen solutions.

each was transferred to a syringe under positive pressure of nitrogen. Stopped-flow experiments were performed in a Durrum-Gibson instrument with a 2 cm light path and a dcad time of 3 msec. All experiments were performed anaerobically at pH 3.0 and 25 °C. The outflow from stopped-flow experiments was collected and the pH monitored. No significant changes from initial values were observed.

Mössbauer Spectroscopy

Rapid freeze: Solutions of iron salts and ligands at concentrations suitable for Mössbauer spectroscopy were prepared as described above. Two syringes, connected with a 'T'-shape capillary tube, were used to mix and transfer the solutions rapidly to a small thin walled polythene Mössbauer cell. The solutions were transferred to the precooled cell and frozen under nitrogen, the total time taken from mixing to freezing was of the order 3–5 seconds. The Mössbauer spectra of the resulting pink solids were recorded at 80 K on the apparatus described by Hamed *et al.* [3] using iron metal as a reference. All the Mössbauer data were computer fitted.

Results and Discussion

Mössbauer Spectroscopy

The Mössbauer data may be conveniently split into two sets of results: those used to establish the stoichiometry of the reaction of iron(III) with GSH (Table I, Fig. 1), and those used to establish the nature of the iron in solution at various times after mixing the metal with the thiol (Table II).

Table I gives the Mössbauer data resulting from frozen solutions, containing 1:1 and 2:1 molar ratios of $FeCl_3$ to GSH. Solutions were frozen after complete reaction. The data from the 1:1 stoichiometry show the presence of iron(II) only; however that from the 2:1 mixture shows the presence of both iron(II) and iron(III). The ratio of iron(II) to iron(III) from the Mössbauer data is about 70:30.

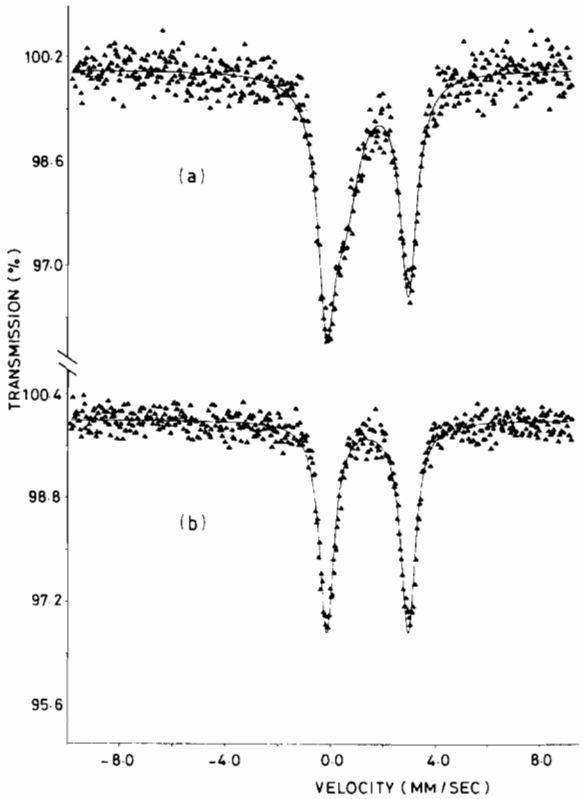

Fig. 1. Mössbauer spectra at 80 K, of a quench frozen solution (a) 2:1 iron(III) chloride to GSH, and (b) 1:1 iron(III) chloride to GSH after complete reaction (see Table I).

This ratio probably underestimates the proportion of iron(III) present due to differences in recoil free fractions between iron(II) and iron(III). These results, allowing for the fact that iron(II) and iron(III) have different 'f' factors and that the 1:1 mixture contains only iron(II) suggests that the stoichiometry of the reaction is as given in Scheme 1.

The Mössbauer spectra provide evidence solely for the final state (B) (in Scheme 1) in which high

TABLE II. Mössbauer Parameters from Spectra Obtained on Quench Frozen Solutions and Solids Containing (either or both) Fe(II) and Fe(III) at 80 K.

Spectrum No.	Mixture	pH	δ mm s^{-1}	Δ mm s^{-1}	Γ mm s^{-1}	Iron Valence Present
1	$FeCl_3$/2GSH (Rapid Freeze) traces of pink [$FeCl_3$] = 0.1 *M*	1.0	1.40(1)	3.19(2)	0.24(1)	Fe^{2+}
2	$FeCl_3$/3GSH [$FeCl_3$] = 0.1 *M*	3.0	1.36(2)	2.98(4)	0.41(3)	Fe^{2+}
3	$FeCl_3$/2Cysteine* (Rapid Freeze) traces of pink [$FeCl_3$] = 0.1 *M*	1.5	1.39(1)	3.10(2)	0.26(1)	Fe^{2+}
4	$FeCl_2 \cdot 4H_2O$/3GSH [Fe] = 0.1 *M*	2.0	1.41(1)	3.15(2)	0.26(2)	Fe^{2+}
5	$FeCl_2 \cdot 4H_2O$/3GSH [Fe] = 0.1 *M*	3.0	1.40(1)	3.08(2)	0.26(1)	Fe^{2+}
6	$FeCl_2 \cdot 4H_2O$/1.5GSSG [Fe] = 0.15 *M*	2.0	1.40(1)	3.12(2)	0.25(1)	Fe^{2+}
7	$FeCl_2 \cdot 4H_2O$/1.5GSSG* [Fe] = 0.15 *M*	3.0	1.38(1)	3.08(1)	0.24(1)	Fe^{2+}
8	$FeNO_3 \cdot 9H_2O$/2GSH‡ (Rapid Freeze) Pink [Fe] = 0.1 *M*	1.5	0.56(2) 1.42(3)	0.72(3) 3.10(5)	0.22(2) 0.22(4)	Fe^{3+} Fe^{2+}
9	$FeNO_3 \cdot 9H_2O$/2GSH (Rapid Freeze) Pink [Fe] = 0.01 *M*	1.5	0.46(3) 1.36(2)	0.63(4) 3.26(3)	0.14(3) 0.20(3)	Fe^{3+} Fe^{2+}
10	$FeNO_3 \cdot 9H_2O$/2GSH† (Colourless) [Fe] = 0.01 *M*	1.5	1.42(1)	3.34(2)	0.21(2)	Fe^{2+}
11	$FeNO_3$/2GSH*‡ $NaNO_3$ (Pink Solid)	–	0.53(3) 1.39(1)	0.68(4) 3.33(2)	0.23(3) 0.18(2)	Fe^{3+} Fe^{2+}
12	$FeCl_3$/GSSG‡ (Reddish-orange) [Fe] = 0.2 *M*	2.0	0.51(2)	0.69(2)	0.20(2)	Fe^{3+}
13	$FeNO_3$/GSSG (Reddish-orange) [Fe] = 0.2 *M*	2.0	0.57(1)	0.65(1)	0.27(1)	Fe^{3+}

*The Fe(II) sites in these spectra are fitted to only one Fe(II) doublet although better fits are found for two Fe(II) or more Fe(II) sites. ‡The Fe(III) sites in these spectra are all fitted as two separate singlets. †This spectrum was obtained by thawing and refreezing the solution which gave spectrum 9.

spin iron(II) in an octahedral environment (possibly distorted) is identified. This high spin environment suggests that the ligands that coordinate to the iron are Cl^- and oxygen of carboxylate groups or water molecules.

This interpretation is supported by chemical analysis of the 2:1 mixture after complete reaction in which 50% of the iron is present in the iron(II) state.

It must be noted that even in the event of rapid freezing equilibria may shift during cooling [6]. If this happens then Mössbauer parameters for the frozen solution reflect the structure not of the initial room temperature solution, but of the solution at the solidification temperature [6].

Table II gives the Mössbauer results of quench frozen solutions of iron(III) nitrate or chloride with GSH or GSSG at pH's 3.0 and below. Spectra 1 and 2 show that the iron valence state of the resulting frozen mass is high spin ferrous, though the actual parameters are different at the different pH values. Spectrum 3 also shows the presence of only high spin ferrous iron in the iron cysteine system. All three spectra indicate that the iron seen by ^{57}Fe Mössbauer spectroscopy is ferrous. These results agree well with those reported by Raudsepp [5], showing GSH reduces iron(III) (as does cysteine as seen in our spectrum 3).

Spectra 4 and 5 of Table II show the results of experiments carried out to examine binding of iron(II) to GSH. The chemical shifts and quadrupole splittings are in the range for materials containing $Fe(OH_2)_4Cl_2$ and $[Fe(OH_2)_6]^{2+}$ octahedra [7–9]. It is obvious that, as these results are so similar to those of spectra 1 to 3, the iron electronic environments as seen from the Mössbauer spectra are also very similar. There is evidence only of oxygen and chloride ligands binding the iron(II) at 80 K. No evidence for sulphur ligand binding is found at this temperature. Such binding might be expected to result in the formation of low spin iron(II).

Spectra 6 and 7 are those that result from quench freezing solutions of iron(II) and GSSG. Again the Mössbauer parameters are similar to those reported in spectra 1–5 and indicate that the iron(II) sites are very similar.

Spectra 1 and 3 were from solutions which were rapidly frozen as soon as possible after mixing. These frozen masses show trace pink colouration but no iron electronic environments were seen other than those given.

Spectra 8 and 9 resulted from rapid freezing of solutions containing $FeNO_3$. These frozen solutions were more intensely pink than those given by $FeCl_3$. The spectra showed the presence of both iron(II) and iron(III). The iron(II) parameters were similar to those found in spectra 1 to 7. The Mössbauer parameters of the ferric iron will be discussed below.

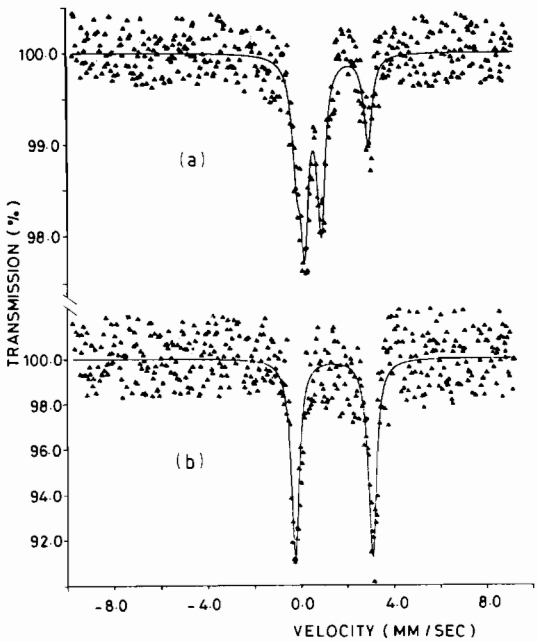

Fig. 2. Mössbauer spectra at 80 K, (a) rapidly frozen solution (pink) of iron(III) nitrate–GSH in a 1:2 proportion, [Fe(III)] = 0.1 *M*, see spectrum 8 Table II, (b) the resultant colourless mass after thawing the pink and re-freezing at 80 °K, see Table II, spectrum 10.

Spectrum 10 is from the material used for spectrum 9 after thawing and refreezing. This procedure resulted in bleaching the pink colour which was accompanied by the disappearance of the iron(III) site.

It would appear that the pink colour is associated with the iron(III) site and that when the reduction goes to completion the iron(III) disappears along with the pink colour (Fig. 2).

It is also of interest that the Mössbauer parameters of this iron(II) site (spectrum 10) are different than those in spectrum 9. Indeed, they are very similar to those reported by Hider *et al.* [9] and are probably due to $[Fe(H_2O)_6]^{2+}$ octahedra as found in $FeCl_2 \cdot 9H_2O$ [7, 8]. Thus in this nitrate solution, on completion of the reduction process at low temperature, the iron(II) is surrounded by six water molecules.

On comparing this latter result with those for the spectra 1–9 it would seem reasonable that in these materials, where the quadrupole splittings are all less than 3.30 mm s^{-1}, part of the GSH or GSSG ligands (possibly oxygen ligands) are still attached to the iron(II).

Indeed, a solid material isolated from solutions containing $FeNO_3$/2GSH and $NaNO_3$ gave a Mössbauer spectrum containing both iron(II) and iron(III) (spectrum 11). Moreover the iron(II) site is similar to that in spectrum 10 suggesting

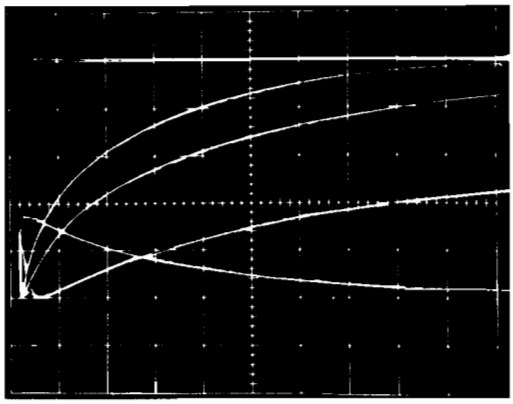

(a)

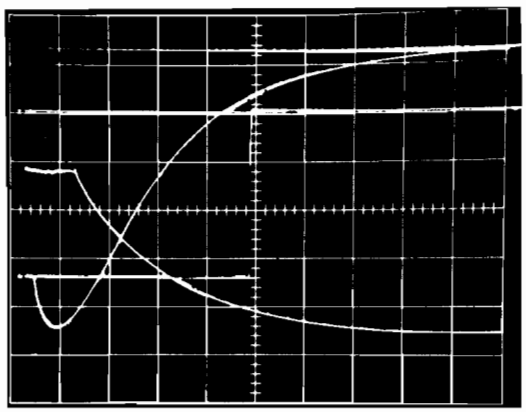

(b)

Fig. 3. Progress curves for the reactions of iron(III) chloride with thiols. Transmittance is presented as a function of time at pH 3.0 and 25 °C. (a) [GSH] = 20×10^{-3} *M* and [Fe(III)] = 5×10^{-3} *M* after mixing. The monitoring wavelength was 625 nm. The sweep times are 2 ms (descending, *i.e.* an increase in absorption) 100 msec, 500 ms and 1 sec per horizontal division and the maximum extinction change was 0.56; (b) [cysteine] = 15×10^{-3} *M* and [Fe(III)] = 1×10^{-3} *M* monitored at 675 nm with sweep times of 5 (descending) and 100 msec per horizontal division and a maximum extinction change of 1.25.

$[Fe(H_2O)_6]^{2+}$ octahedra. The iron(III) site is similar to that of spectra 9, 12 and 13. As this material contains iron, nitrate, GSSG and H_2O, the iron(III) site might well be expected to be similar to those of spectra 12 and 13 which contain $FeCl_3$ and $FeNO_3$ respectively with GSSG.

As the material in spectrum 9 is eventually reduced to give spectrum 10 then this iron(III) site must be due to an iron(III) and GSH environment. This environment is, from the Mössbauer data, electronically similar to that of iron(III) and GSSG. This point is discussed later when the overall reaction mechanism is considered.

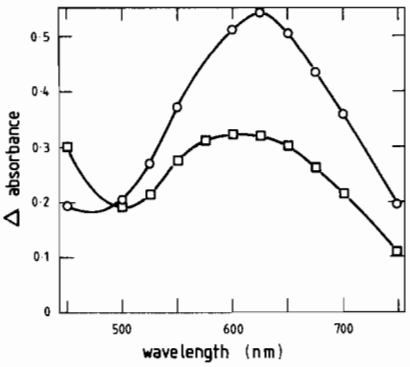

Fig. 4. The calculated absorbance spectra of the blue complexes Spectra were calculated from progress curves (○) 20 msec and (□) 500 msec after mixing. [GSH] = 15×10^{-3} *M* and [Fe(III)] = 5×10^{-3} *M* after mixing. The temperature was 25 °C, slit width 0.5 mm.

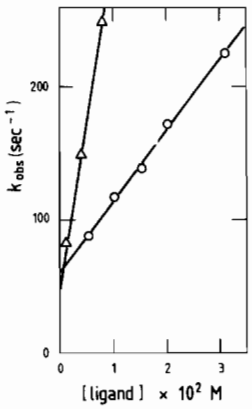

Fig. 5. Ligand concentration dependence of k_{obs} for the formation of the blue complex is shown as a function of ligand concentration, (△) N-acetyl cysteine, [Fe(III)] = 1×10^{-3} *M* after mixing and (○) GSH, [Fe(III)] = 5×10^{-3} *M* after mixing at pH 3.0 and 25 °C.

Reactions of Reduced Glutathione with Ferric Iron at Low pH

Mössbauer studies (above) indicated that in aqueous acidic solution, ferric iron was reduced under anaerobic conditions to the ferrous state. In the presence of both chloride and nitrate it was possible to produce, at liquid nitrogen temperatures, frozen solutions which were pink in colour. On raising the temperature, this colour disappeared yielding the normal colourless final product.

It is clear that complex formation and electron transfer reactions must both play a role in the overall mechanism.

Stopped-flow Experiments

In order to examine the properties of intermediates and obtain rate data to elucidate mechanism, we performed rapid mixing experiments in a

TABLE III. Maximum Absorbance Changes at 625 nm for the Blue Complexes Formed for Different Thiols. The binding constants, the complex concentrations and the values of ϵ were calculated as described in the text.

Ligand No.	Ligand	[L] molar	[Metal] molar	$\Delta A_{(625\,nm)}$ (2 cm light path)	k_1 M^{-1} s^{-1}	[Complex (I)]$_{max}$ molar	Apparent binding Constant (approx) (K M^{-1})	ϵ (M^{-1} cm^{-1}) (approx)
1	GSH	15×10^{-3}	1×10^{-3}	0.202				
	GSH	15×10^{-3}	5×10^{-3}	0.560	5.2×10^3	2.5×10^{-3}	100	110
2	Cysteine	15×10^{-3}	1×10^{-3}	1.25				
3	N-Acetyl cysteine	15×10^{-3}	1×10^{-3}	1.22	2.7×10^4	0.9×10^{-3}	600	650
4	Cysteine Methyl ester	15×10^{-3}	1×10^{-3}	0.17				
5	Mercapto ethanol	15×10^{-3}	1×10^{-3}	0.21				

stopped-flow apparatus. On mixing reduced glutathione with ferric chloride at pH 3 we observed a very rapid increase in absorbance in the long wavelength region of the visible spectrum *i.e.* the rapid formation of a blue compex, which then decayed in a slower process yielding finally a colourless product in agreement with the Mössbauer studies. A typical progress curve for these processes is reported in Fig. 3.

By performing this experiment at a number of wavelengths it was possible to build up the absorption spectrum of the blue intermediate(s). Figure 4 shows the spectra of the reaction medium at 20 ms and 500 ms after mixing. In both cases the spectra obtained were very broad with peaks at 625 nm and approximately 590 nm respectively. These spectra are not identical and this indicates the presence of at least two intermediates (both blue) in the pathway. This conclusion is also supported by the biphasic nature of the decay process reported in Fig. 3a.

The rate of the rapid first process (Fig. 3) was found to depend on the concentration of both iron and GSH. Figure 5 shows the dependence of this rate on GSH concentration under pseudo first order conditions, holding the initial iron(III) concentration constant. This behaviour is consistent with a mechanism in which GSH and iron(III) come together in a second order reaction leading to the production of a blue complex. No evidence, however, is provided by this experiment as to whether the production of this complex also involves an electron transfer step, although the Mössbauer studies (above) indicate that relatively early in the reaction, *i.e.* before the blue complex has time to decay, iron(II) has been formed. The simplest formulation for the first step would therefore be of the form:

$$Fe(III) + GSH \underset{k_{-1}}{\overset{k_1}{\rightleftharpoons}} Complex\ (I) \qquad (1)$$

Figure 5 allows us to estimate the value of k_1 as 5.2×10^3 M^{-1} s^{-1} from the slope of the line while a value for k_{-1} of 60 s^{-1} is obtained from the intercept*. Thus the value of the apparent equilibrium constant for formation is approximately 100 M^{-1}.

A similar value for the association constant was obtained by monitoring the change in absorption at the wavelength maximum of the blue complex (I) (625 nm) as a function of GSH concentration. Figure 6a shows the results of such an experiment and it is

*Strictly this procedure is incorrect as we depart from pseudo-first order conditions at low glutathione concentrations. However in other experiments where the ratio of Fe(III) to glutathione was maintained while the absolute concentrations were varied a more formally correct analysis yielded a value for k_1 of 5.5×10^3 M^{-1} s^{-1}.

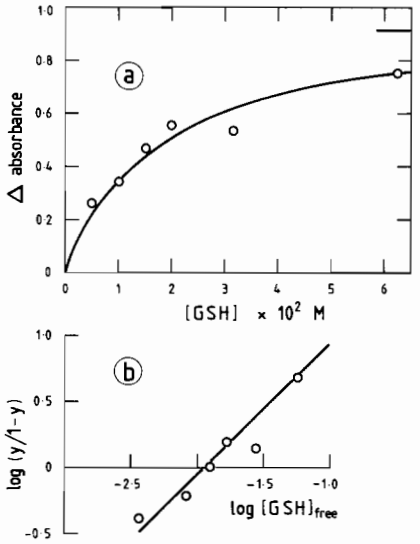

Fig. 6. Amplitude of maximum absorbance change as a function of glutathione concentration. a) Amplitudes of maximum absorbance changes from progress curves, as shown in Fig. 1, plotted against glutathione concentration. The iron(III) concentration was 5×10^{-3} *M*; other conditions as for Fig. 3. The solid line is a hyperbolic binding curve asymptotically approaching the horizontal line. b) Hill plot of the data given in (a), where Y is the fractional saturation estimated from (a) by dividing the Δabsorbance by 0.91, the estimated Δabsorbance for infinite [GSH].

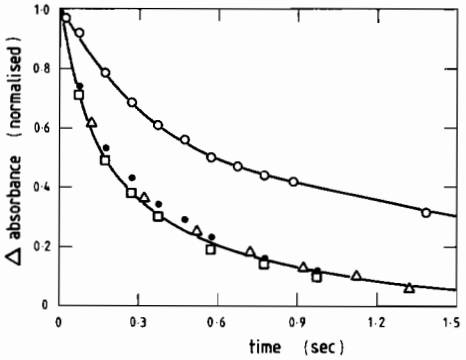

Fig. 7. A plot of normalized absorbance *versus* time for the decay of the blue complex as a function of GSH concentrations. The solid lines are thoretical curves of the form: Absorbance = $Ae^{-k_1 t} + Be^{-k_2 t}$ where A and B are the proportions of each phase in the decay profile and k_1 and k_2 are the rate constants of each phase. [GSH] 0.25 *M* (•); 0.0625 *M* (△); 0.0313 *M* (□) and 0.02 *M* (○). A, B, k_1 and k_2 have the values 0.5, 0.5, 8.6, 1.5 s^{-1} respectively for 0.25 *M*, 0.0625 *M* and 0.0313 *M* [GSH]. The comparable values for 0.02 *M* GSH are 0.4, 0.6, 3.5, 0.56 s^{-1}. The iron concentration was 5×10^{-3} *M*.

apparent that the hyperbolic curve obtained is in agreement with the simple formulation of equation (1). The apparent binding constant may be determined from this data by a Hill plot, (Fig. 6b) which conforms to a simple binding process with a Hill coefficient of unity and an association constant of 100 M^{-1}.

Using the value of 100 M^{-1} derived from the kinetic experiments for the apparent equilibrium constant for binding, and knowing the initial concentrations of GSH and $FeCl_3$, it is possible to estimate the concentration of complex (I) in solution immediately following the rapid initial reaction. With this information and the absorbance change monitored in the stopped-flow spectrophotometer we obtained a value for the extinction coefficient at 625 nm for this complex. This value, together with that calculated on a similar basis for N-acetyl cysteine is given in Table III.

Decay of the Blue Complex (Complex (I))

The decay of the blue complex (I) proceeds, as stated above, via at least one other complex in a biphasic process. The rates of these processes were determined by assuming that each conforms to an exponential decay under the conditions employed (Fig. 7).

Figure 7 illustrates the time dependences of the decay of the blue complex (I) under a variety of GSH concentrations. It is evident that over a wide range of concentrations the normalized profiles may be simulated by the sum of two exponentials of equal magnitude. The relative sizes of these together with their rate constants are concentration independent down to approximately 30 m*M* GSH; this indicates that the decay of complex (I) is rate limited by first order reactions possibly involving ligand exchange processes and rearrangements (see later). At below 30 m*M* GSH, the profile, even when normalised to the same absorbance, showed a distinct change in shape. The faster part (Fig. 7) possibly conforms to the same sum of exponentials as discussed but with an additional very slow process becoming evident. The relative magnitude of this very slow step in the decay increased with decreasing GSH concentration. We interpret this as a change in mechanism of the decay processes at low GSH concentrations.

Reaction of Ferric Iron with Other Thiols

Glutathione may provide a number of ligands to ferric iron at low pH, *e.g.* thiol, amino nitrogen and two carboxylate groups.

In order to obtain evidence as to which of these sites is bound to the iron in the coloured intermediates, and to compare the effect of ligand on the reduction process, we have repeated the experiments described above with the following thiol derivatives; (a) mercapto ethanol, (b) L-cysteine, (c) N-acetylcysteine, (d) cysteine methyl ester.

TABLE IV. Comparison of Ligand Effect on k_{obs} (Pseudo First Order Rate Constant) for the Formation of the Blue Complex.

Ligand No.	Ligand	[L] × 10^{-3} *M*	[Metal] × 10^{-3} *M*	k_{obs} s^{-1}
1	GSH	4.15	1.0	66
	GSH	15.0	5.0	138
2	L-cysteine	15.0	1.0	106
3	N-Acetyl cysteine	3.9	1.0	145
	N-Acetyl cysteine*	7.8	1.0	247
5	Mercapto ethanol	15.0	5.0	78

*At 15 × 10^{-3} *M* N-Acetyl cysteine concentration the formation of the blue complex was very fast and within the dead time of the stopped-flow apparatus.

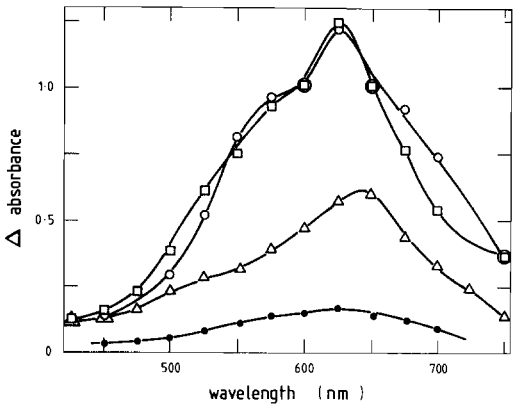

Fig. 8. The absorbance spectra for the blue transient obtained with different thiols. (□) [cysteine] = 15 × 10^{-3} *M*, [Fe(III)] = 1 × 10^{-3} *M*; (○) [N-acetyl cysteine] = 15 × 10^{-3} *M*, [$FeCl_3$] = 1 × 10^{-3} *M*; (△) [mercaptoethanol] = 15 × 10^{-3} *M*, [$FeCl_3$] = 5 × 10^{-3} *M*; (●) [cysteine methyl ester] = 15 × 10^{-3}, [$FeCl_3$] = 1 × 10^{-3} *M* at pH 3.0 and 25 °C.

All the compounds studied rapidly produced a blue complex when mixed with $FeCl_3$. The rate of this process (Table IV) varied with the nature of the thiol derivative being slowest for mercapto ethanol and fastest for N-acetyl cysteine, (Fig. 5), the second order ratc constants for the latter being 2.7 × 10^4 M^{-1} s^{-1}.

The difference spectra of the complexes formed are shown in Fig. 8. It is apparent that while the overall spectral distribution is similar, if not identical, for each compound, the intensity of the absorption band λ_{max} (see Table III) was strongly dependent on the nature of the thiol. This variation may be due to either or both of two factors, *viz.*:

(a) differences in the complex concentrations due to the ligand dependence of the binding constant for complex formation (see eqn. 1).

(b) ligand dependence of the extinction coefficient of the complex.

Whereas it is not possible, as yet, to disentangle these factors completely and unambiguously we have attempted to do so in the cases of GSH and N-acetyl cysteine. The kinetic experiments depicted in Fig. 5 allow us to make estimates of the values of the binding constants (as described above for GSH). From these and with a knowledge of the initial concentrations we have calculated the maximum concentration of complex attained and hence, by comparing these with the absorbance changes to estimate the values of ϵ. Table III shows the results of these calculations. It is apparent when comparing GSH and N-acetyl cysteine, that both the extinction coefficient and the value of K (apparent) increase by a factor of approx. 6 fold.

These experiments also allow us to determine the initial iron binding sites of the ligands. The thiol function is the group all compounds have in common as a binding site. The similarity of the reaction between cysteine and N-acetyl cysteine would seem to exclude the involvement of the amino group in binding. All the ligands may offer an oxygen site either as a carboxyl, hydroxyl, or ester function, and we propose that oxygen co-operates with the thiol function to give the intense blue complex (I). The stereochemistry of the ligand and the nature of the oxygen (either COO^-, COOR or OH) may be expected to influence the binding constant and hence the intensity of the complex (see Table III and above discussion). The probable binding sites offered by each ligand and their possible mode of chelation in forming the initial blue complex (I) are presented in Table V.

The decay of complex (I) is also ligand dependent. The decay profiles were biphasic for GSH and mercapto ethanol while they were monophasic for cysteine and its derivatives. Also the decay rate was much faster for the cysteine and N-acetylcysteine. Figure 9 shows the concentration dependence of this decay rate. We note the change in rate limit from a second order to a first order process on increasing N-acetyl cysteine concentration is consistent with ligand exchange processes playing

TABLE V.

Ligand No.	Ligand	Structure in solution at pH 3	Possible chelating sites at pH 3	Iron Complex (I)	Ring sizes
1	Glutathione	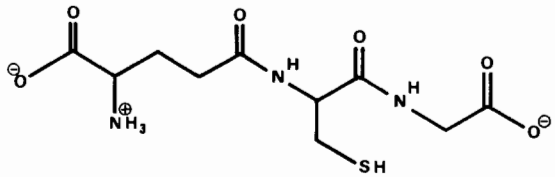	COO^-(Gly) COO^-(Glu) NH(Gly) NH(Cys) SH	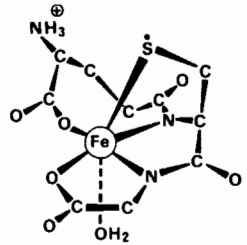	5,5,6,8
2	L-Cysteine	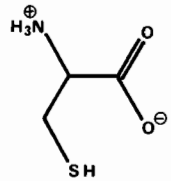	COO^- SH	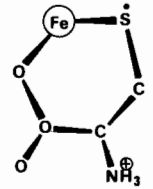	6
3	N-Acetyl cysteine	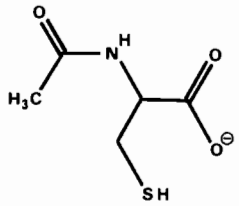	COO^- SH	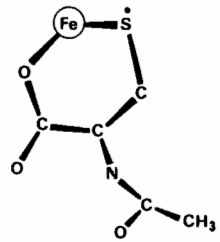	6
4	Cysteine methylester	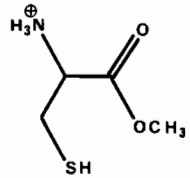	$COOCH_3$ SH	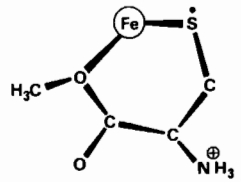	6
5	Mercaptoethanol	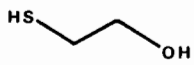	OH SH	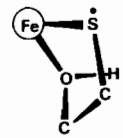	5

Section 1 $Fe(III) + (GS)^- \underset{k_{-1}}{\overset{K_1 \; k_1}{\rightleftharpoons}} [Fe(III)(GS)]^{2+} \underset{\Delta H^\circ \text{ neg}}{\overset{K_2}{\rightleftharpoons}} \left[\begin{matrix} \dot{S}\text{–}Fe(II) \\ | \\ G \end{matrix} \right]^{2+}$

(Pink?)

Complex (I)
Blue

Section 2 

2 × Complex (I)

†Ligands to iron(II) may include (a) carboxylate or SH groups from the excess GSH present, or (b) carboxylate groups donated from the final product GSSG.; The full complement of ligands is provided by ligands which stabilize high spin iron(II) *e.g.* Cl, H_2O

Scheme 1

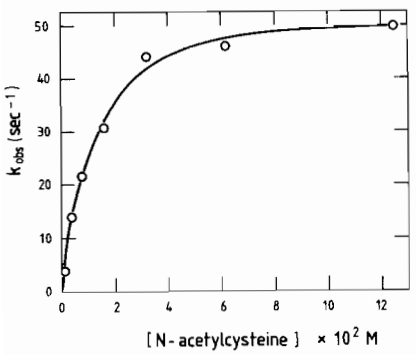

Fig. 9. The ligand concentration dependence of rate constant for the decay of the blue transient calculated under first order conditions, for N-acetyl cysteine. $[FeCl_3] = 1 \times 10^{-3}$ *M*. Other conditions as for Fig. 3.

a role in the production of the final product.

Conclusions and Remarks

In agreement with a previous report [4], we note the production of complexes on mixing ferric iron salts with glutathione. However, in contrast with this earlier investigation we show here that the final product of the reaction, if carried out anaerobically is iron(II). Also we report here that the initial binding (and electron transfer reaction) is very rapid leading to a blue intermediate. This is also at variance with the earlier work [4] and we believe that this discrepancy may have arisen through Khan and Langford misinterpreting the slow decay process as the initial binding reaction.

We believe that the Mössbauer and the kinetic data presented are consistent with an overall reaction pathway as depicted in Scheme I.

For clarity we shall discuss parts of this mechanism in turn and attempt to relate the steps involved to our experimental findings.

Section 1 of this scheme indicates the formation of a 1:1 $(GS)^-Fe(III)$ complex which is followed by a very rapid electron transfer reaction to form the blue complex (I) which contains iron(II) and a glutathione radical. At 25 °C the concentration of the ferric intermediate is very small and is not observable. The stopped flow experiments show that the formation of complex (I) is rate limited by a second order step (k_1) and it is this value we report in Table III.

As the ferric intermediate is at low concentration at 25 °C, Section I collapses (in the kinetic sense) to the simple formation given above in eqn. 1.

The apparent equilibrium constant (K_{app}) which is quoted for the formation of complex (I) is therefore a function of both the binding constant K_1 and the redox equilibrium constant K_2 and approximates to $K_1 \cdot K_2$.

Experiments in which glutathione and iron(III) salts were mixed and rapidly frozen showed no blue colour, although this could be detected visually prior to freezing. Freezing occurred in a time which from the kinetic observations would allow complex (I) to be trapped at least partially. These frozen solutions were in fact pink and if rapidly thawed in hot water exhibited a transient blue colour, detectable visually prior to final bleaching. The intensity of the pink colouration depended on the nature of the anion, being most noticeable for nitrate and less

intense for chloride. Mössbauer studies, particularly with the nitrate salt clearly showed the presence of iron(III). We interpret these results in terms of the temperature and anion dependence of the value of K_2.

On lowering the temperature to 80 K, the redox equilibrium is perturbed in favour of the ferric intermediate (an enthalpy of ~2 Kcal/mol would be sufficient). The greater intensity of the pink colour and the presence of significant amounts of iron(III), in the nitrate containing solution, is in agreement with the greater affinity of chloride for iron(II) at low temperatures. Thus chloride tends to stabilize iron(II) while nitrate, a non-coordinating species, allows easy temperature reversal of the redox equilibrium.

Section 2 depicts the decay of blue complex (I) to the final products. These are iron(II), as demonstrated by Mössbauer spectroscopy, and presumably as GSH is the reducing species it itself must be oxidized to GSSG. There are certainly a number of steps involved in the decay process but as GSSG is considered to be formed it implies that dimerisation must be involved. The stopped-flow experiments indicate that, with GSH at least, one other intermediate is in the pathway.

Although at this time we are unable to identify the number and nature of the intermediates we are able to say something about the rate limiting processes. It is clear that over a range of glutathione concentration, the decay process is concentration independent (Fig. 7) indicating that at least one first order step, possibly a rearrangement or ligand dissociation, is involved. At lower GSH concentrations the decay profile is altered indicating that a second order step involving either excess GSH or possibly the GSSG product and an intermediate(s) in the path, must be present and is now the rate limiting step.

The rate constants for these decay processes depend upon the nature of the thiols under consideration. For example, the decay of the blue complex formed with N-acetyl cysteine is much more rapid (than with GSH), but also indicates the presence of both first and second order steps leading to the final products (Fig. 9).

Finally, let us turn our attention to the nature of the glutathione ligands that are binding iron by comparison with the data obtained from other thiols.

The intensity of the blue complexes formed in the cases of L-cysteine and N-acetyl-L-cysteine with iron are of the same order but the rate of formation is faster with the latter compound (Tables III and IV).

We explain this observation by noting that the former compound (2) (Table V) could have an intramolecular H-bond between the $NH_3^{\oplus}$ and the negatively charged carboxyl group so that the net attraction for iron will be less than for N-acetyl-L-cysteine (compound 3) which would not have this hydrogen bond. Compounds 1, 4 and 5 (Table V) all show a less intense blue than do compounds 2 and 3 (see Table III). Compounds 4 and 5 do not carry a negatively charged oxygen while GSH (compound 1) has three likely iron-binding groups on the cysteine and glycine residues (Table V) namely sulphur, carboxylic acid and NH(Gly). These may give rise to two chelate rings (of 5 and 6 atoms) which may cause strain and slow binding though the carboxylate groups in this molecule are charged. The carboxylate of the glutamyl residue will obviously be able to bind the iron but because of the large resulting ring size involved, we expect this to be slower. Indeed, the rate of formation of the GSH/iron blue complex is slower than that of compounds 2 and 3 which supports these arguments. We note that in the known structure of Cu–GSSG [12] all these ligands and the NH_2 of the glutamyl residue are bound to copper at high pH. (The copper complex is prepared at high pH.)

In 90% ethanol a blue iron(III) complex of L-cysteine with similar structural and physical properties to that in Table V has been reported [13]. However, reduction of the iron was not considered.

References

1 'Glutathione. A Symposium'. Academic Press, New York, 1954.
2 D. L. Rabenstein, R. Guevremont and C. A. Evans, 'Metal Ions in Biological Systems', vol. 9, H. Sigel, Ed., Dekker, New York, Chapter 4 (1979).
3 M. Y. Hamed, R. C. Hider and J. Silver, *Inorg. Chim. Acta, 66,* 13 (1982).
4 T. R. Khan and C. H. Langford, *Can. J. Chem., 54,* 3192 (1976).
5 R. Raudsepp, *Eesti Nsv Tead. Akad. Toim., Fuus., Mat., 24(3),* 312 (1975).
6 A. Vertes, L. Kovecz and K. Burges, 'Mössbauer Spectroscopy', Elsevier, Amsterdam, Oxford, New York, Chapter 3 (1979).
7 S. L. Ruby, B. L. Zabransky and J. G. Stevens, *J. Chem. Phys., 54,* 11 (1971).
8 S. L. Ruby and B. L. Zabransky, *Chem. Phys. Letts., 13,* 382 (1972).
9 R. C. Hider, A. R. Mohd-Nor, J. Silver, I. E. G. Morrison and L. V. C. Rees, *J. Chem. Soc., Dalton Trans.,* 609 (1981).
10 A. J. Nozik and M. Kaplan, *J. Chem. Phys., 49(9),* 4141 (1968).
11 I. Dezsi, L. Keszthleyi, L. Pocs and L. Korecz, *Phys. Letts., 14(1),* 14 (1965).
12 K. Miyoshi, Y. Sugiura, K. Ishizu, Y. Litaka and H. Nakamura, *J. Am. Chem. Soc., 102,* 6130 (1980).
13 A. Tomita, H. Hirai and S. Makishima, *Inorg. Chem., 7,* 760 (1968).